Journal of Computing and Electronic Information Management
ISSN: 2413-1660 | Vol. 11, No. 1, 2023

Finite Element 3D Simulation Experiment on Shield Excavation

Xinggui Shi

School of Civil Engineering and Architecture, Wenzhou Polytechnic, Wenzhou 325000, China

Abstract: Shield technology is widely used in subway excavation projects, and the excavation of soil causes surface settlement, which affects the normal use and safety of the tunnel itself and surface buildings. Using Abaqus, a large general-purpose finite element software, a three-dimensional excavation finite element model of the shield tunnel is established, and the dynamic excavation process of the shield tunnel is finely simulated to derive the soil displacement settlement law during the shield excavation, and to discuss the influence of the change of the simulated values of the post-shield grouting pressure and support pressure on the maximum settlement (uplift) of the ground surface. The conclusions of the study have important theoretical and practical engineering significance.

Keywords: Shield technology; Finite element; 3D.

1. Introduction

Three-dimensional finite element analysis has been widely used for shield tunneling simulation, which can reflect the spatial properties of the ground displacement caused by shield tunneling construction and can reflect the tunneling process comprehensively. However, due to the complexity and uncertainties of the shield construction process, it is difficult to accurately consider the soil stratification, material nonlinearity, soil pressure in the shield sealing chamber, groundwater, construction voids at the end of the shield, and simultaneous grouting behind the shield wall, while the contact between the structure and the soil is less involved, which is still a topic that needs to be studied in depth.

2. Project Overview

The shield tunnel has a circular cross-sectional shape and is a single-layer lining structure consisting of precast reinforced concrete pipe pieces assembled in a ring shape. The outer diameter of the ring lining is 4.8 m, the thickness is 0.3 m, and the width is 0.9 m. The lining ring consists of five standard blocks and one arch base block. The top of the tunnel is 9.6 m above the ground surface, and there are three soil layers above the bedrock, namely soil layer 1 (8 m), soil layer 2 (8 m), and soil layer 3 (16 m). The Duncan-Chang principal parameters of each soil layer are shown in Table 1, where the density unit of γ is kN/m3. The concrete lining structure uses a linear elastic model with a design basic strength of σck=42N/mm2 and a modulus of elasticity of 3.25MPa, which is used in this paper to simulate the tunnel lining using a homogeneous circle, while the actual tunnel lining is assembled by joints, to consider the influence of this part on the stiffness, the modulus of elasticity of the lining is discounted to 2.64 MPa, Poisson's ratio is 0.167, and the weight is 26 kN/m3. The groundwater level is 2m above the ground, and the water-earth calculation is used.

Table 1. Soil material parameters

Location of soil layer	γ	c (KPa)	φ (°)	R_f	K	n	K_b	m	G_{max}
Soil layer 1	18.5	15	19	0.9	110.7	0.75	99.6	0.68	2.47×10^7
Soil layer 2	18	13	19	0.98	155.7	0.71	140.3	0.64	3.1×10^7
Soil layer 3	19	32	25.8	0.87	110.7	0.65	88.6	0.52	1.21×10^8

3. Finite element fine simulation

3.1. Model Building

The calculation area is taken as 48m, the actual thickness of the soil layer is taken as 32m in the depth direction, and the axial direction is taken as 100m.

The model boundary conditions are as follows: along the tunnel axis, horizontal constraints are applied to the front and rear boundary nodes; vertical horizontal constraints are applied to the nodes on the symmetry plane; vertical horizontal constraints are applied to the right boundary of the model; vertical constraints are applied to the nodes at the bottom of the model.

The contact stresses and relative displacements between the liner and the surrounding soil are simulated using a master-slave contact surface model. The grid cells of the soil surrounding the tunnel were encrypted, and the grid of the soil far from the tunnel chamber was gradually increased to meet

the research needs and save computing time. A total of 15783 nodes and 12642 cells were manually meshed as shown in Figure 1.

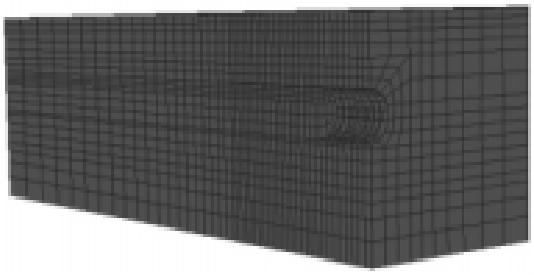

Figure 1. Schematic diagram of finite element model

3.2. Finite element excavation simulation

The tunnel excavation process not only changes the geometry of the object but also changes the stresses and deformations of the remaining structure. From previous studies, it is known that the tunnel excavation process is accompanied by unloading effects that lift. The stress and deformation of the excavation effect can be expressed by the following equation: $\{\Delta\ \delta_1^1\}=-\{\ \delta_1^1\}$, $\{\Delta\ \sigma_1^1\}=-\{\ \sigma_1^1\}$; $\{\ \delta''\}=\{\ \delta_2^1\}+\{\ \delta_2^2\}+\{\Delta\delta 2\}$, $\{\ \sigma''\}=\{\ \sigma_2^1\}+\{\ \sigma_2^2\}+\{\Delta\sigma 2\}$; $\{\delta 2\}=\{\Delta\delta 2\}$, $\{\sigma\}=\{\sigma_2^2\}$. The key issue is how to use finite element software to simulate the characteristics of different stages of tunnel excavation, so that the stress on the excavation surface is completely relieved and becomes stress free.

3.2.1. Calculation of initial equilibrium

The initial displacement is assumed to be zero and the initial stress field is the soil self-weight stress field. By applying the effective stress field to the soil unit under its weight and by adding the self-weight load to the soil unit, the soil is in equilibrium and obtains an initial displacement of the order of 10-3 m. This state is considered to be the initial state of the tunnel excavation.

3.2.2. Soil excavation

The shield advance is studied as a discontinuous process, and it is assumed that the shield is advanced step by step in a hopping manner, and the length of each advance (longitudinal) is the width of one lining unit. Therefore, in this paper, it is assumed that the soil advances 0.9 m per excavation. A uniform load (0.15 MPa) is applied to the excavated soil unit surface to simulate the support pressure outside the excavation. The momentary unsupported state of the surrounding soil after the liner is released from the shield tail is simulated by releasing part of the nodal reaction force from the soil body. By using the unit generation technique, the lining unit is generated to form the soil-lining interaction system, and finally the equilibrium reaction force is released to zero. The backing grouting is simulated using the equivalent uniform force method with a value of 0.05 MPa. The above three steps are equivalent to the completion of an excavation, and the simulation of the shield tunnel advance is repeated until the surface settlement value stabilizes.

4. Analysis of finite element calculation results

4.1. Final settlement and displacement analysis of the soil

After 24 excavation steps, the shield was analyzed by taking the ground surface as shown in Fig. 2, the outer surface in the vertical tunnel direction and the outer surface along the tunnel direction for the final settlement displacement in the vertical direction, as shown in Fig. 2(B), 2(A) and 2(C) respectively (unit: m).

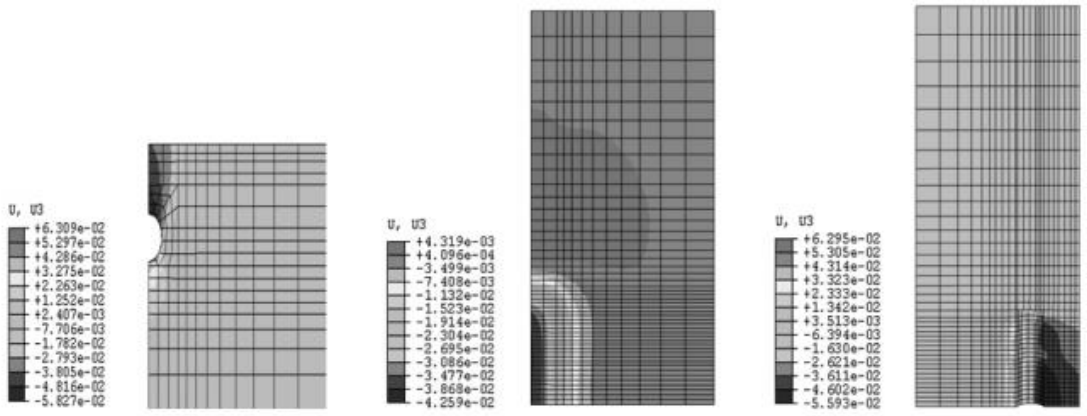

A) Outer surface in vertical tunnel direction B) Ground surface C)The outer surface along the tunnel direction

Figure 2. Final Settlement Displacement Analysis

The soil behind the tunnel excavation is the unloading area, and the soil in front of the excavation is disturbed to cause stress release, which is then balanced by the support pressure at a close distance. However, in practice, the support pressure cannot be taken to be the same as the pressure in the soil ahead. If the pressure is slightly higher, the soil in front of the shield will bulge, because as the shield moves forward, the forward soil builds up in front of the excavation, and the cutter prevents the soil from deforming into the tunnel, causing the ground to bulge. This uplift will eventually lead to a larger settlement in the tunnel, which will be further discussed in the study on the effects of the model parameters.

As can be seen in Figure 2(A), the maximum transverse ground settlement displacement due to tunnel excavation occurs in the soil above the central axis of the tunnel, and then gradually decreases as the soil moves away from the tunnel excavation, reaching 6.5 m with little effect on the ground settlement.

Figure 2(B) also shows that the settlement of the soil above the tunnel axis increases with the depth of the soil layer.

As can be seen in Figure 2(C), the soil above the tunnel axis sinks with a maximum value of 55.9 mm, while below the

axis it rises with a maximum value of 62.95 mm. For the soil below, the weight of the lining is much less than the weight of the original soil due to the excavation and the stress relief caused by the pore space at the end of the shield. These factors mean the process of unloading for the soil below, so it causes the soil to bounce up.

From the above three figures, it can be seen that the soil displacement during the shield construction has a clear three-dimensional character with a large variation of horizontal and vertical displacement of the soil around the tunnel at different locations along the tunnel transverse and longitudinal directions.

4.2. Analysis of the 20th excavation step

The analysis of the excavation process was carried out to determine the excavation step (step 20) by taking the ground surface as shown in Figure 1, the outer surface in the vertical tunnel direction, and the outer surface along the tunnel direction for the vertical final settlement displacement analysis, as shown in Figure 3(B), Figure 3(A), and Figure 3(C), respectively (unit: m).

Comparing Fig. 3(A) and Fig. 2(A), the final settlement (step 24) and step 20 are the same, with a difference of 0.52 mm or 1% in the maximum settlement. Figure 3(B) shows that the tunnel excavation has almost no effect on the displacement of the soil 40 m away from the front, and Figure 2(B) also shows that the tunnel excavation does not affect on the soil 40 m away from the front. A comparison between Figure 3(B) and Figure 2(B) and between Figure 3(C) and Figure 2(C) also shows that the settlement pattern and the magnitude of the values are basically the same. It can be considered that the settlement pattern, vertical size, and the area and size of the soil affecting the front can be reasonably judged in 24 steps of excavation, and the soil settlement has stabilized. To save calculation time and computer memory, it is reasonable to excavate 24 steps (two shield body lengths) in this paper.

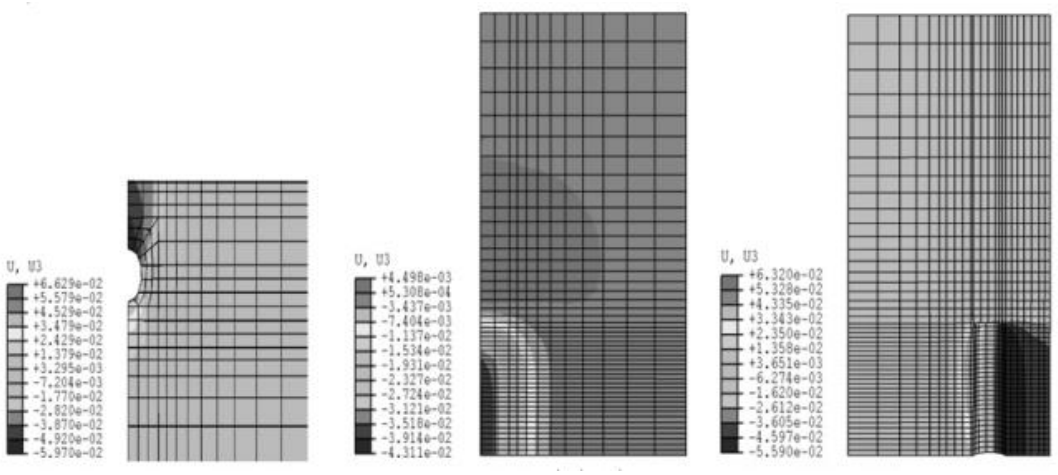

D) Outer surface in vertical tunnel direction E) Ground surface F) The outer surface along the tunnel direction

Figure 3. Step 20 Displacement Settlement

4.3. Timing analysis of a characteristic point

According to the excavation plan, the shield is excavated to the section where this point is located in step 3. Before the third step of excavation, this point is in the soil in front of the excavation, and there is a small amount of elevation due to the pressure of the excavation surface; as the shield arrives at the operation, the soil is disturbed and starts to settle slightly, and when the shield passes and the shield tail leaves this point, the stresses in the gap at the end of the shield are released and the soil is further disturbed causing a large settlement of the soil; finally the soil gradually approaches a stable value. The settlement pattern of this characteristic point is consistent with the description of related literature.

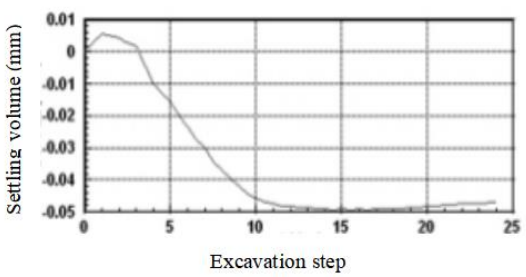

Figure 4. Feature point time course curve

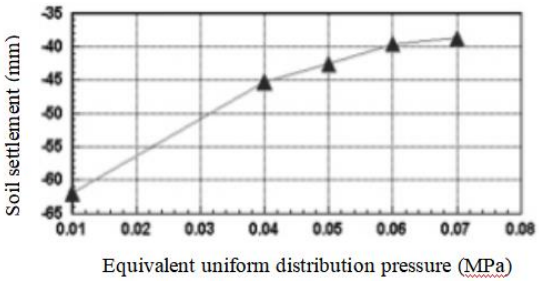

Figure 5. Relationship between uniform pressure and maximum settlement displacement

4.4. Study on the influence of model parameter changes

(1) Influence of grouting values behind the shield, some studies show that grouting with or without simulation has a great influence on the surface settlement, while the actual slurry has a liquid-to-solid change process, which is difficult

to simulate accurately, and the simulation method adopted in this paper assumes the same pressure values in the four grouting holes, which further increases the error of the results. In this paper, we further analyze the effect of the equivalent uniform pressure on the surface settlement displacement by using the method of the equivalent uniform pressure, with all other parameters unchanged, and simulating the effect of the equivalent uniform pressure of 0.07MPa, 0.06MPa, 0.05MPa, 0.04MPa and 0.01MPa respectively. The calculation shows that the surface displacement settlement decreases gradually with the increase of grouting pressure, and it is noted that the settlement value does not change very much between 0.04MPa and 0.07MPa, only a 6mm difference, which does not have a great impact on the construction. The method is also worthy of reference. The maximum displacement value increases to 63 mm when the value of 0.01 MPa is taken, and the difference is 24 mm, or 50%, from the value of 0.07 MPa. It can be assumed that as the value of the mean pressure decreases, it is getting closer to the case without considering the grouting pressure, so the error can be large and even cause errors in the numerical simulation method. In practice, the grouting pressure should not be too high, for the steel pipe lining piece, the grouting pressure will deform the pipe ring, followed by the main beam and the ribs, and for the concrete lining piece, the bolts will be sheared off. The grouting pressure must be chosen with great care, and should not be increased unrestrictedly to reduce settlement displacement.

(2) Influence of the support pressure value, like the grouting pressure value, the support pressure value is also very difficult. In most cases, according to the engineering practice, the experts concerned use the full discussion of the stratigraphic conditions to determine the upper and lower values and set the management pressure within the range. However, as the amount of excavation and the deformation of the stratum change, the value will be increased or decreased appropriately. In this paper, numerical simulations were performed for 0.2MPa, 0.15MPa and 0.1MPa, 0.05MPa for the support pressure. The effect of the change of this value on the soil uplift (settlement) in front of the excavation and the soil settlement behind the excavation are shown in Fig. 6 and Fig. 7, respectively.

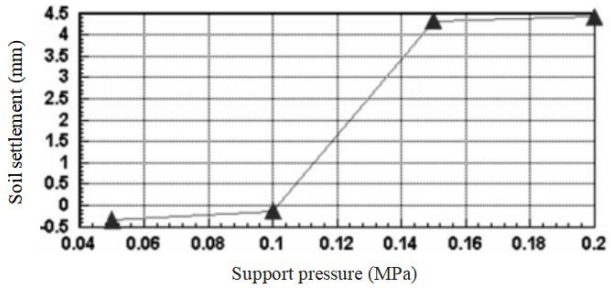

Figure 6. Relationship between support pressure and maximum uplift (settlement) of the soil in front

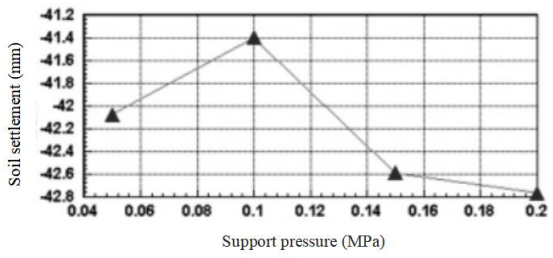

Figure 7. Relationship between support pressure and maximum settlement of the back soil

As the support pressure decreases, the soil uplift gradually decreases, and when the support pressure continues to decrease, the soil settles in front of the body.

The data show that when the support pressure is close to the real soil pressure, the settlement value of the soil behind is the smallest. This phenomenon can be explained according to the theory in the literature when the support pressure is greater than the true soil pressure, it will disturb the soil in front of the excavation and cause the soil at the excavation face to extrude in front of the excavation face, and the displacement of the soil at the excavation face will further cause the settlement; while when the support pressure is less than the true soil pressure, the soil will collapse in the direction of the shield machine, resulting in the loss of stratum, and finally causing the settlement value of the soil surface to become larger. However, the support pressure does not have a great influence on the settlement of the soil behind, so it is unrealistic to reduce the surface displacement settlement by changing the support pressure.

5. Conclusion

In this paper, the mechanical mechanism of tunnel excavation was described and some theoretical conclusions were made to guide the numerical modeling and analysis of the 3D finite element shield excavation. A three-dimensional numerical model of the shield tunneling process was developed using Abaqus finite element software and Inp keyword commands. The model takes into account soil stratification, material nonlinearity, the interaction between the soil and lining structure, earth pressure in the shield sealing chamber, and construction voids at the end of the shield. Due to the lack of actual measurement data, the model results can only be compared and analyzed with the existing universal laws and empirical formulas. The analysis shows that the finite element calculation results of this thesis have good regularity. To save computer memory and computation time, this paper considers that the 24 steps of excavation can satisfy the judgment and analysis of the regularity of the results and the anticipation of the regularity of the subsequent excavation steps. For the actual shield excavation and numerical simulation, it is relatively difficult to obtain the values of post-shield grouting pressure and excavation surface support pressure.

References

[1] J.Yuan. Finite element analysis of surface and soil deformation induced by shield construction [D]. Tianjin: Tianjin University, 2008. (in Chinese)

[2] A.Z Lu, B.S Jiang, C.A. You. Research on the range of finite element mesh division in displacement inverse Analysis [J]. Chinese Journal of Civil Engineering, 1999, 32(1): 26-30.

[3] F.X. Zhang, H.H Zhu, D.M. Fu. Shield tunnel [M]. Beijing: People's Communications Press, 2004.

[4] Y.LI.Three-dimensional numerical simulation and experimental study of shield construction deformation [D]. Tianjin: Tianjin University, 2004.

[5] W.B. Zhou, Shield Tunnel Construction Technology and Application [M]. Beijing: China Building and Construction Press, 2004.

[6] J.H. Qian, Z.Z. Yin Geotechnical Principles and Calculation [M]. Beijing: Water Resources and Hydropower Press, 2nd edition, 1996

[7] K.M. Lee, R. K. Rowe. An analysis for three- dimensional ground movements.the Thunder Bay tunnel[J]. Canada Geotech, 1991, 28:25-41.

[8] Finno.R.J, Clough. G.W. Evaluation of Soil R esponse to EPB Shield Tunnelling[J]. Journal of Geotechnical Engineering, 1985,111(2): 157-173.

[9] B.F. Zhu Principle and Application of Finite Element Method [M]. Beijing: China Water Resources and Hydropower Press, 1998.

[10] X. Zhang, X.L. Ding, S.C. Li Secondary development of Duncan-Chang Model in Abaqus Finite Element Analysis software [J]. Journal of Yangtze River Scientific Research Institute, 2005,18(4): 46-51.